IEEE Access
Multidisciplinary : Rapid Review : Open Access Journal

Received January 13, 2020, accepted January 27, 2020, date of publication February 3, 2020, date of current version April 30, 2020.

Digital Object Identifier 10.1109/ACCESS.2020.2971135

A Broadband Planar Spiral Antenna Design for Electromagnetic Signal Monitoring

DAIFU CHEN[1], **HONGXIN ZHANG**[1], **AND JUN XU**[2]
[1]Electrical Engineering Department, Beijing University of Posts and Telecommunications, Beijing 100876, China
[2]Beijing Institute of Spacecraft System Engineering, Beijing 100086, China

Corresponding author: Hongxin Zhang (hongxinzhang@bupt.edu.cn)

This work was supported in part by the National Natural Science Foundation of China under Grant 61571063, in part by the Beijing Natural Science Foundation under Grant 3182028, and in part by the Fundamental Research Funds for the Central Universities (BUPT) under Project 2019XD17 and Project 2019PTB-001.

ABSTRACT In order to meet the wide-band full-space radio monitoring task, the design of a circular-polarized planar dual-arm composite spiral antenna is presented in this paper. The antenna operation covers the L-band and S-band frequencies ranging from 200 MHz to 6 GHz (relative bandwidth is 187.1%). The equiangular spiral is applied to the beginning of the Archimedean spiral, which reduces the input impedance of the antenna, thereby reducing the length of the cross-section of the feed balun and realizing the miniaturization of antenna. The antenna is designed to be simple in structure and small in size. The diameter of the radiating surface and the length of the section are only 1/5 and 1/50 of the working wavelength. The simulated and measured results show that the antenna has a very good impedance matching (standing wave ratio of less than 2.5), and the antenna has good symmetry, and has good circular polarization and wideband characteristics. Finally, the antenna is applied with an USRP (universal software radio peripheral) to carry out the electromagnetic signal monitoring experiment outdoors. The results show that the designed antenna can receive electromagnetic signals in the 200 MHz - 6 GHz band and can be used for full-space radio monitoring.

INDEX TERMS Circular polarization, low profile, miniaturization, planar helical antenna, ultra-wideband.

I. INTRODUCTION

With the widespread application of Ultra-wideband antenna in the field of mobile communication, planar helical antenna has been widely studied for its advantages of broadband, simple structure, circular polarization and low cost [1]–[3]. However, the volume of the planar helical antenna is limited by the working frequency, and the size of the low frequency antenna is always too large [4]. Therefore, it has important engineering value for the miniaturization design of planar spiral antenna.

At present, the miniaturization technology of planar helical antenna has been studied a lot. In general, antenna miniaturization mainly includes aperture miniaturization and profile miniaturization [5]–[8]. The miniaturization of aperture is mainly due to the innovation of antenna radiation structure, such as the tortuous processing of the antenna arm in the radiation belt, the improvement of low frequency radiation effect, and the reduction of antenna diameter [9]–[11]. In addition, the composite antenna is also an important miniaturization method, such as the equal angle helix and Archimedean spiral combined sky line, and the antenna terminal loading lumped resistance [12]–[14]. The realization of low profile is mainly achieved by adding absorbing materials to the reflector, using EBG (Electromagnetic Band Gap) structure as the reflector, special-shaped reflector and bending balun.

In this paper, a planar composite helical antenna with low input impedance at 200 MHz - 6 GHz is proposed. The radiation surface diameter of the antenna is $0.2\lambda_{max}$ and the profile depth is $0.02\lambda_{max}$. Under the same working band 200 MHz - 6 GHz, the diameter of the Archimedean spiral antenna requires at least $0.4\lambda_{max}$, while the diameter of the equiangular spiral antenna is at least $0.5\lambda_{max}$ [15], [16]. Compared with the traditional planar spiral antenna, the diameter of the antenna is reduced by 50% and 60% by means of the combination of the equal angle helix and the Archimedean spiral, and the diameter of the antenna is miniaturized. By analyzing the principle of exponential

The associate editor coordinating the review of this manuscript and approving it for publication was Lu Guo.

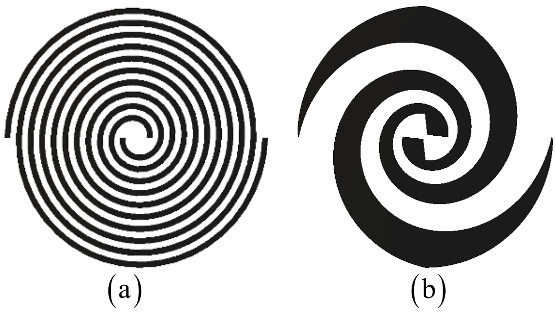

FIGURE 1. Spiral structures.

gradient microstrip line, the smaller the input impedance of the antenna is, the smaller the balun length is. In this paper, the designed antenna input impedance is 75 Ω, and its corresponding balun length is only 30 mm, which realizes miniaturization of the antenna.

II. ANTENNA DESIGN

Planar helical antennas usually have two forms: the helix antenna and the isometric spiral antenna. As shown in Fig.1 (a), the radius of the antenna increases uniformly with the change of angle, and its equation is formula (1):

$$r = r_0 + a(\varphi - \varphi_0) \tag{1}$$

Here r_0 is spiral starting radius; φ is the azimuth; φ_0 is the starting angle; a is the spiral growth rate; (r, φ) is the polar coordinate of any point on the curve. The arm's Archimedean antenna is a zoned radiation, and a spiral band with a circumference of about one wavelength forms the effective radiation band of the antenna. The antenna diameter needs at least $0.4\lambda_{max}$.

As shown in Fig.1 (b), the shape of an equiangular helical antenna is completely determined by its angle, and its curve equation is equation (2):

$$r = r_0 \cdot e^{a(\varphi - \varphi_0)} \tag{2}$$

Here r_0 is spiral starting radius; φ is the azimuth; φ_0 is the starting angle; a is the spiral growth rate; (r, φ) is the polar coordinate of any point on the curve. An isometric antenna is an ultra-wideband antenna. When the length of the spiral arm is greater than one wavelength, the antenna begins to exhibit non-frequency characteristics, and the antenna diameter needs at least $0.5\lambda_{max}$.

In order to realize the miniaturization of the antenna aperture, a composite slot spiral antenna is designed, as shown in Fig.2. The inner ring of the antenna is an isometric spiral, and the outer ring is an Archimedean spiral. The whole antenna has the characteristics of an isometric helical antenna, that is, the spiral arm length will be non-frequency-changing after being longer than one wavelength, and the outer ring has a small antenna length due to the Archimedean spiral, and the antenna is still small size. At the same time, in order to minimize the size of the antenna, the antenna is designed as a slot spiral structure.

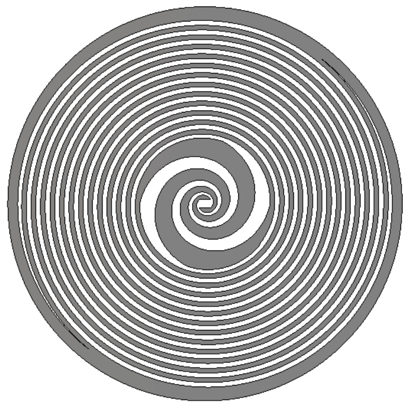

FIGURE 2. Composite slot spiral antenna structure.

The parametric equation of the inner boundary curve of the equiangular helix is:

$$\begin{cases} X(t) = \left[r_0 \cdot e^{a_1 * (\varphi - \varphi_0)}\right] \cdot \cos(t) \\ Y(t) = \left[r_0 \cdot e^{a_1 * (\varphi - \varphi_0)}\right] \cdot \sin(t) \\ 0 \le t \le n_1 \cdot 2\pi \end{cases} \tag{3}$$

The parametric equation of the outer boundary curve of the equiangular helix is:

$$\begin{cases} X(t) = \left[r_0 \cdot e^{a_1 \cdot (\varphi - e - \varphi_0)}\right] \cdot \cos(t) \\ Y(t) = \left[r_0 \cdot e^{a_1 \cdot (\varphi - e - \varphi_0)}\right] \cdot \sin(t) \\ 0 \le t \le n_1 \cdot 2\pi \end{cases} \tag{4}$$

The parametric equation of the outer boundary curve of the Archimedean spiral is:

$$\begin{cases} X(t) = \left[r_0 \cdot e^{a_1 \cdot n_1 \cdot 2\pi} + a_2 \cdot t\right] \cdot \cos(t) \\ Y(t) = \left[r_0 \cdot e^{a_1 \cdot n_1 \cdot 2\pi} + a_2 \cdot t\right] \cdot \sin(t) \\ n_1 \cdot 2\pi \le t \le n_2 \cdot 2\pi \end{cases} \tag{5}$$

The parametric equation of the inner boundary curve of the Archimedean spiral is:

$$\begin{cases} X(t) = \left[r_0 \cdot e^{a_1 \cdot n_1 \cdot 2\pi} + a_2 \cdot t + w\right] \cdot \cos(t) \\ Y(t) = \left[r_0 \cdot e^{a_1 \cdot n_1 \cdot 2\pi} + a_2 \cdot t + w\right] \cdot \sin(t) \\ n_1 \cdot 2\pi \le t \le n_2 \cdot 2\pi \end{cases} \tag{6}$$

The model is built and optimized in the electromagnetic simulation software CST according to the parametric equation. On the basis of maintaining good working characteristics of the antenna (ie, S11 curve, gain, and axial ratio), the structural parameters of the antenna are comprehensively adjusted to reduce the input impedance of the antenna to 75 Ω, thereby miniaturizing the antenna profile. The composite slot spiral antenna is designed to use a FR4 substrate with a thickness of 1.6mm and a relative dielectric constant $\varepsilon_r = 4.3$. The structural parameters are shown in Table 1.

III. EXPONENTIAL GRADIENT BALUN

The structure of a planar helical antenna is balanced and symmetric, and an exponential transformation balun is often

TABLE 1. **Design values.**

Parameters	Values
r_0	1.5 mm
a_1	0.221
φ_0	0
n_1	1.4
e	75
a_2	1.07
w	1.7 mm

TABLE 2. **Design values.**

Parameters	Values
w_1	1.49 mm
w_2	1.9 mm
w_3	9.5 mm
l	30 mm

used to achieve impedance matching and balanced feeding between the antenna and the coaxial line. According to the principle of impedance transformation of the exponential gradient line, the shortest length of the balun satisfies the formula (7).

$$l_{\min} = \frac{\lambda_0}{8\pi \varepsilon_r \left|\Gamma_L\right|} \left|\ln \frac{Z_L}{Z_0}\right| \tag{7}$$

Among them, Z_L is the antenna input impedance, Z_0 is the coaxial line impedance, ε_r is the dielectric constant of the antenna dielectric plate, λ_0 is the wavelength of the lowest frequency of the antenna operation, and Γ_L is the terminal reflection coefficient. From equation (7), the shortest length of the exponential gradient balun is limited by the minimum operating frequency of the antenna and the input impedance.

In order to reduce the antenna volume and reduce the length of the antenna profile, the input impedance of the antenna is designed to be 75 Ω. The designed balun uses a FR4 material with a thickness of 1mm and a relative dielectric constant $\varepsilon_r = 4.3$ as the balun dielectric substrate. The structure is shown in Fig.3. The specific parameters are shown in Table 2.

According to the above parameters, the model is built and simulated in the CST, and the simulation results of the return loss and the balun transmission coefficient of the balun unbalanced end are obtained, as shown in Fig.4. In the 200 MHz - 6 GHz frequency band, the transmission coefficient of the balun is greater than −0.5 dB, and the return loss of the unbalanced end is less than −10 dB, which satisfies the antenna feeding requirement.

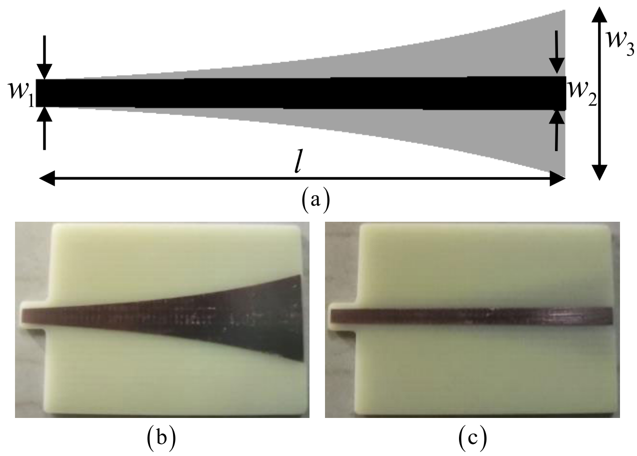

FIGURE 3. **(a) Structure of the proposed exponential gradient balun. (b) Top view of the fabricated balun. (c) Bottom view of the fabricated balun.**

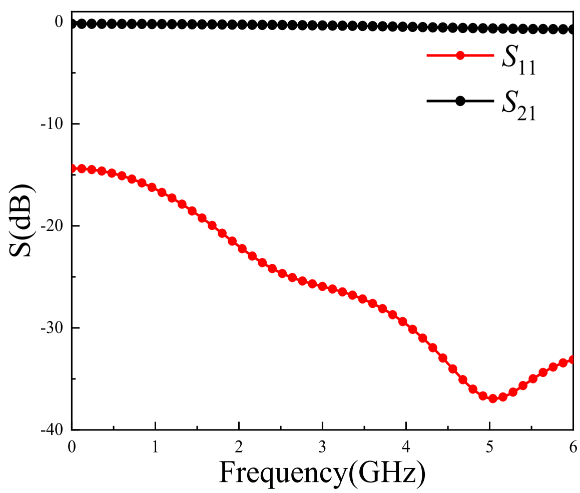

FIGURE 4. **Balun simulation result.**

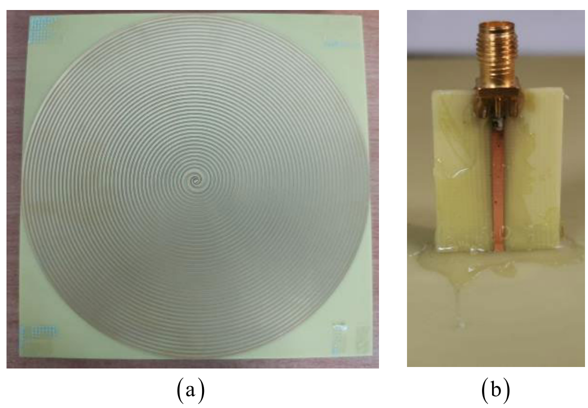

FIGURE 5. **Fabricated antenna. (a) Top view of the antenna. (b) Side view of the antenna.**

IV. SIMULATION AND MEASUREMENT RESULTS

In order to verify the proposed design, a prototype of the antenna is fabricated and tested. The fabricated antenna is shown in Fig.5. The impedance characteristics of the proposed wideband antenna are then evaluated throughout the range of the operating frequencies through measurements in an anechoic chamber using vector network analyzer.

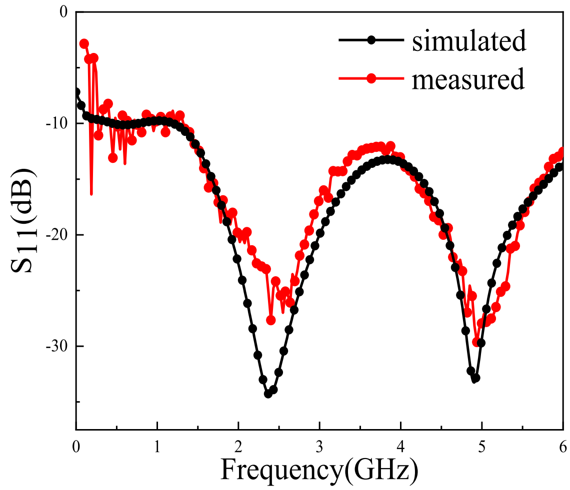

FIGURE 6. Measured and simulated S_{11} of antenna.

The measured results are compared with the simulations to validate the experiment.

Comparison of the simulated and measured S_{11} responses of the proposed planar spiral antenna in free space is given in Fig.6. The simulated results agree very well with the measurements confirming it can be considered as a broadband antenna. The antenna achieves a −10 dB impedance bandwidth of 5.9 GHz in simulation (ranging from 0.1 GHz to 6.0 GHz) and 5.8 GHz in measurement (ranging from 0.2 GHz to 6.0 GHz). Small discrepancies present between the two results are most likely associated to the fabrication tolerances.

Fig.7 shows the antenna gain angle measured in a microwave anechoic chamber, where θ and φ are the zenith angle from the positive z-axis in the spherical coordinate system and the azimuth angle from the positive x-axis in the xy plane, respectively. Since it is a circularly polarized antenna, there are no E plane and H plane, so two vertical planes of $\varphi = 0°$ and $\varphi = 90°$ are taken for analysis. The results are shown for both RHCP and LHCP radiated fields in two different ($\varphi = 0°$ and $\varphi = 90°$) planes are almost harmonized. In the broadside direction, the RHCP components are approximately 20 - 30 dB greater than the LHCP components which indicates that the antenna has notable right hand circular polarization purity. It is verified that the shortening of the exponentially graded microstrip balun does not affect the feed performance of its unbalanced-balance.

Fig.8 presents the comparison of simulated and measured axial ratio results of the proposed planar spiral antenna along the direction of maximum radiation. The measured and simulated results of the axial ratio are almost matched. The proposed antenna efficiently achieves the 3 dB axial ratio in the whole of the region of 0.2 GHz to 6.0 GHz. Minimum axial ratio is 0.3 dB at 4 GHz in simulation and 0.4 dB at 0.5 GHz in measurement while its maximum value is 2.9 dB at 5 GHz in simulation and 2.3 dB at 6 GHz in measurement. Overall, a very good circular polarization bandwidth is expressed

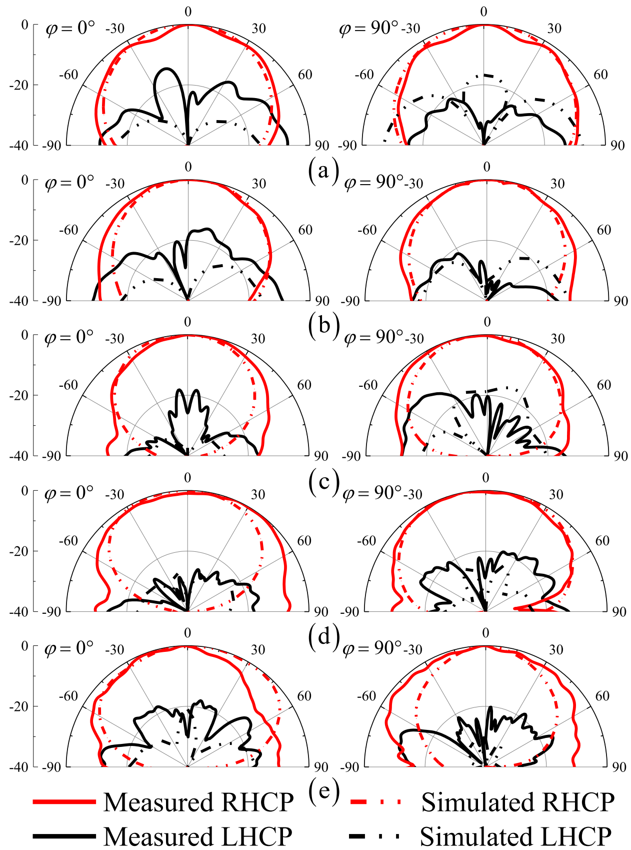

FIGURE 7. Measured and simulated radiation patterns. (a) 0.5 GHz. (b) 1 GHz. (c) 2 GHz. (d) 3 GHz. (e) 4 GHz.

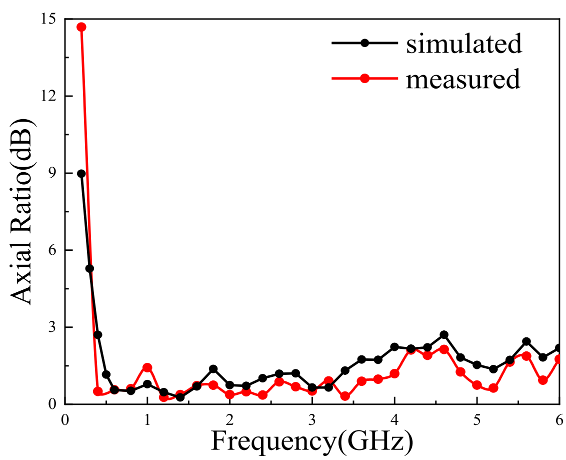

FIGURE 8. Measured and simulated axial ratios and gains of the proposed antenna.

by the antenna both in simulation and measurement, which meets the radiation requirements of circular polarization of antenna.

Fig.9 shows the gain of the antenna in the main radiation direction versus frequency. In the frequency range of 200 MHz - 6 GHz the gain of the antenna increases with the increase of frequency, and the orientation is better,

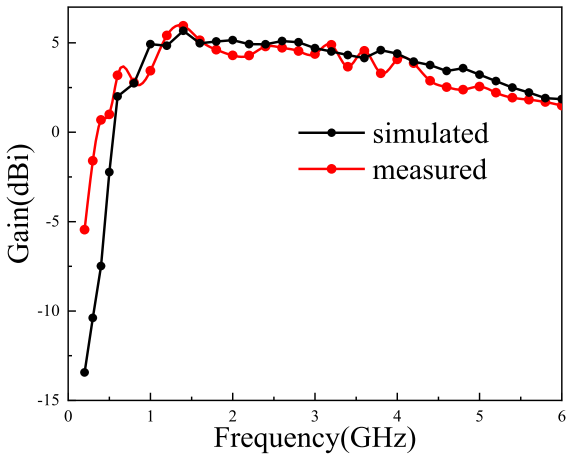

FIGURE 9. Gain of the proposed antenna.

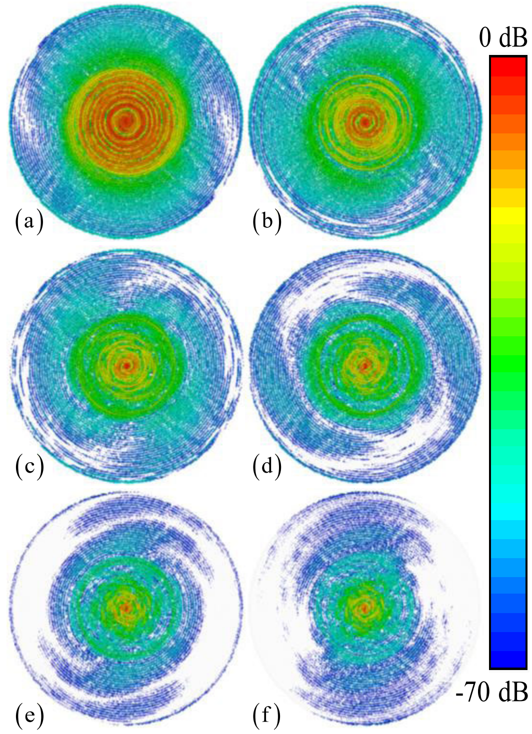

FIGURE 10. Surface current of the antenna. (a) 0.5 GHz. (b) 1 GHz. (c) 2 GHz. (d) 3 GHz. (e) 4 GHz. (f) 5 GHz.

which meets the requirements of miniaturized and wide-band receiving antenna. The lowest gain at the lowest frequency point is mainly limited by the antenna aperture.

The balun and the antenna model are integrated into the CST for simulation, and the surface current distribution map of the antenna at 6 frequency points can be obtained, as shown in Fig.10. It can be seen that for each frequency point, the magnitude of the current on the spiral arm is gradually attenuated from the center of the spiral to the outer region,

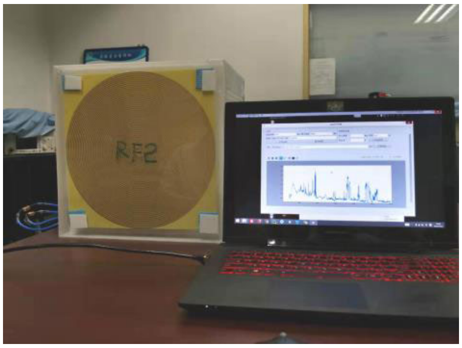

FIGURE 11. Antenna is used to monitor environmental signals.

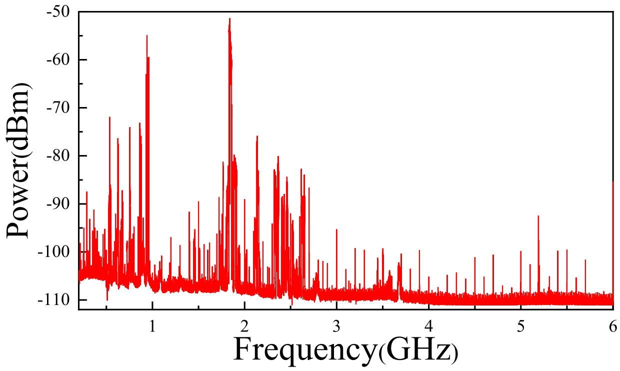

FIGURE 12. Environmental spectrogram.

which indicates that the standing wave on the spiral arm is small and the antenna has a low axial ratio characteristic.

Table 3 presents a comparison between the proposed antenna and state-of-the-art spiral antenna designs for microwave segment operation reported in open literature. Size is calculated considering lowest operating frequency reported in these studies. The comparison shows that the proposed antenna achieves the maximum relative bandwidth (relative bandwidth is 187.1%) compared to all reported designs. At the same time, the proposed design also achieves the lowest operating frequency (200 MHz), and has an overall smaller size and lower profile.

V. USRP MEASUREMENT WITH ANTENNA

In order to verify the actual use of the antenna in the monitoring equipment, the antenna and the USRP-N210 instrument are assembled into an electromagnetic monitoring device, as shown in Fig.11.

The equipment is placed in an external field environment to monitor the electromagnetic waves of the surrounding environment. The sweep spectrum monitoring signal is shown in Fig.12.

From the experimental results, the spectral map of the output can clearly display the electromagnetic signal within 200 MHz - 6 GHz. The designed antenna can meet the requirements of environmental electromagnetic monitoring equipment for detecting unknown strong signals.

TABLE 3. Comparison of spiral antennas.

Ref. no.	S_{11} bandwidth (GHz)	AR bandwidth (GHz)	Gain (dBi)	Electrical dimensions (λ_m)	relative bandwidth (%)
[7]	1 ~ 10	2 ~ 10	-10 ~ 9.5	0.31 × 0.31 × 0.1	163.3
[8]	0.5 ~ 3.5	0.5 ~ 2.5	-5 ~ 5	0.42 × 0.42 × 0.08	133.3
[9]	1.9 ~ 8.5	2 ~ 6	-10 ~ 7.5	0.22 × 0.22 × 0.13	126.9
[10]	2 ~ 18	-	-6 ~ 7	0.87 × 0.87 × 0.02	160.0
[11]	3.95 ~ 10.6	3 ~ 12	1.5 ~ 5	0.79 × 0.79 × 0.015	91.4
[12]	0.8 ~ 3	1.5 ~ 3	-10 ~ 5	0.38 × 0.38 × 0.19	115.8
[13]	2 ~ 18	2 ~ 18	-2 ~ 6	0.35 × 0.38 × 0.106	160.0
[14]	0.8 ~ 4.37	0.9 ~ 4.37	7.5 ~ 13	0.30 × 0.30 × 0.15	138.1
[17]	2.5 ~ 4.5	2.5 ~ 4.5	3.5 ~ 5	0.32 × 0.32 × 0.083	57.1
[18]	6 ~ 16	6 ~ 16	5.2 ~ 9.6	1.68 × 1.68 × 0.16	90.9
This work	0.2 ~ 6	0.4 ~ 6	-3 ~ 6	0.20 × 0.20 × 0.02	187.1

VI. CONCLUSION

This paper proposes a new antenna design for environmental electromagnetic monitoring equipment, which is applied to the working frequency range of 200 MHZ - 6 GHZ, and its performance is studied. The slot-composite spiral method simplifies and miniaturizes the antenna structure. In addition, an unbalanced-balanced impedance conversion balun with a gradually changing index from microstrip line to parallel two lines is also designed in this paper, so that the antenna maintains wideband characteristics and circular polarization characteristics. The measured results show that the antenna has a wide band of 5.8 GHZ, and the impedance matching performance is better than −10 dB, which is suitable for wireless electromagnetic monitoring applications.

REFERENCES

[1] D. Muller and K. Sarabandi, "Design and analysis of a 3-arm spiral antenna," *IEEE Trans. Antennas Propag.*, vol. 55, no. 2, pp. 258–266, Feb. 2007.

[2] T.-Y. Shih and N. Behdad, "A compact, broadband spiral antenna with unidirectional circularly polarized radiation patterns," *IEEE Trans. Antennas Propag.*, vol. 63, no. 6, pp. 2776–2781, Jun. 2015.

[3] B. Kramer, M. Lee, C.-C. Chen, and J. Volakis, "Design and performance of an ultrawide-band ceramic-loaded slot spiral," *IEEE Trans. Antennas Propag.*, vol. 53, no. 7, pp. 2193–2199, Jul. 2005.

[4] L.-J. Xu, Y.-X. Guo, and W. Wu, "Miniaturised slot antenna for biomedical applications," *Electron. Lett.*, vol. 49, no. 17, pp. 1060–1061, Aug. 2013.

[5] Q. Liu, C.-L. Ruan, L. Peng, and W.-X. Wu, "A novel compact archimedean spiral antenna with gap-loading," *Progr. Electromagn. Res. Lett.*, vol. 3, pp. 169–177, 2008.

[6] A. Alex-Amor, P. Padilla, J. M. Fernández-González, and M. Sierra-Castañer, "A miniaturized ultrawideband Archimedean spiral antenna for low-power sensor applications in energy harvesting," *Microw. Opt. Technol. Lett.*, vol. 61, no. 1, pp. 211–216, Jan. 2019.

[7] C. Liu, Y. Lu, C. Du, J. Cui, and X. Shen, "The broadband spiral antenna design based on hybrid backed-cavity," *IEEE Trans. Antennas Propag.*, vol. 58, no. 6, pp. 1876–1882, Jun. 2010.

[8] E. A. Etellisi, M. A. Elmansouri, and D. S. Filipovic, "Wideband monostatic simultaneous transmit and receive (STAR) antenna," *IEEE Trans. Antennas Propag.*, vol. 64, no. 1, pp. 6–15, Jan. 2016.

[9] Y.-W. Zhong, G.-M. Yang, J.-Y. Mo, and L.-R. Zheng, "Compact circularly polarized archimedean spiral antenna for ultrawideband communication applications," *IEEE Antennas Wireless Propag. Lett.*, vol. 16, pp. 129–132, 2017.

[10] W. Fu, E. R. Lopez, W. S. T. Rowe, and K. Ghorbani, "A planar dual-arm Equiangula spiral antenna," *IEEE Trans. Antennas Propag.*, vol. 58, no. 5, pp. 1775–1779, May 2010.

[11] T. W. Eubanks and K. Chang, "A compact parallel-plane perpendicular-current feed for a modified equiangular spiral antenna," *IEEE Trans. Antennas Propag.*, vol. 58, no. 7, pp. 2193–2202, Jul. 2010.

[12] J. M. O'Brien, J. E. Grandfield, G. Mumcu, and T. M. Weller, "Miniaturization of a spiral antenna using periodic Z-plane meandering," *IEEE Trans. Antennas Propag.*, vol. 63, no. 4, pp. 1843–1848, Apr. 2015.

[13] N. Rahman and M. N. Afsar, "A novel modified archimedean polygonal spiral antenna," *IEEE Trans. Antennas Propag.*, vol. 61, no. 1, pp. 54–61, Jan. 2013.

[14] S. M. H. Ranjbaran and S. Mohanna, "Improved spiral antenna with a new semi-fractal reflector for short-range sensing," *IET Microw., Antennas Propag.*, vol. 12, no. 11, pp. 1839–1845, Sep. 2018.

[15] J. Kaiser, "The Archimedean two-wire spiral antenna," *IRE Trans. Antennas Propag.*, vol. 8, no. 3, pp. 312–323, May 1960.

[16] J. Dyson, "The equiangular spiral antenna," *IRE Trans. Antennas Propag.*, vol. 7, no. 2, pp. 181–187, Apr. 1959.

[17] T. Pan, L. Dai, S. Chen, Z. Yan, and Y. Lin, "Low-impedance flexible archimedean-equiangular spiral antenna," *IEEE Antennas Wireless Propag. Lett.*, vol. 18, no. 9, pp. 1789–1793, Sep. 2019.

[18] H. H. Tran and T. T. Le, "Ultrawideband, high-gain, high-efficiency, circularly polarized Archimedean spiral antenna," *AEU-Int. J. Electron. Commun.*, vol. 109, pp. 1–7, Sep. 2019.

DAIFU CHEN was born in Jingzhou, Hubei, China, in 1997. He received the master's degree in electronic information engineering from the Wuhan University of Science and Technology, in 2014. He is currently pursuing the master's degree in electronic communication engineering with the EMB and EMC Laboratory, Beijing University of Posts and Telecommunications. His research interests include antenna design, electromagnetic waves, and electromagnetic signal processing.

HONGXIN ZHANG was born in Binzhou, Shandong, in 1969. He received the Ph.D. degree from the Beijing University of Posts and Telecommunications, in 2004. He is a Professor with the Beijing University of Posts and Telecommunications. He is currently a Doctoral Tutor with the Beijing University of Posts and Telecommunications and the Director of the Center for Broadband Communications and Microwave Technology. His research interests include wireless communication and electromagnetic compatibility, communication signal processing, electromagnetic radiation, information security, biomedical engineering, and so on.

JUN XU was born in Kunming, China, in 1982. He received the B.S. degree in telecommunications engineering and the Ph.D. degree in electromagnetic field and microwave technology from the Beijing University of Posts and Telecommunications, Beijing, in 2005 and 2010, respectively. He is currently a Senior Engineer with the Beijing Institute of Spacecraft System Engineering. His research interests include electromagnetic computation and EMC in aerospace.